Island Arc (2009) **18**, 293–305

Thematic Article

Regional-Scale Excess Ar wave in a Barrovian type metamorphic belt, eastern Tibetan Plateau

TETSUMARU ITAYA,[1]* HIRONOBU HYODO,[1] TATSUKI TSUJIMORI,[2] SIMON WALLIS,[3] MUTSUKI AOYA,[4] TETSUO KAWAKAMI[5] AND CHITARO GOUZU[6,7]

[1]*Research Institute of Natural Sciences, Okayama University of Science, Okayama 700-0005 (itaya@rins.ous.ac.jp),* [2]*Pheasant Memorial Laboratory, Institute for Study of the Earth's Interior, Okayama University, Tottori 682-0193,* [3]*Department of Earth and Planetary Sciences, Graduate School of Environmental Studies, Nagoya University, Nagoya, 464-8602,* [4]*Institute of Geology and Geoinformation, National Institute of Advanced Industrial Science and Technology (AIST), Tsukuba 305-8567,* [5]*Department of Geology and Mineralogy, Graduate School of Science, Kyoto University, Kyoto, 606-8502,* [6]*Open Research Center, Okayama University of Science, Okayama 700-0005, and* [7]*Hiruzen Institute for Geology & Chronology, Okayama 703-8248, Japan*

Abstract Laser step heating $^{40}Ar/^{39}Ar$ analysis of biotite and muscovite single crystals from a Barrovian type metamorphic belt in the eastern Tibetan plateau yielded consistent cooling ages of ca. 40 Ma in the sillimanite zone with peak metamorphic temperatures higher than 600°C and discordant ages from 46 to 197 Ma in the zones with lower peak temperatures. Chemical Th-U-Total Pb Isochron Method (CHIME) monazite (65 Ma) and sensitive high mass-resolution ion microprobe (SHRIMP) apatite (67 Ma) dating give the age of peak metamorphism in the sillimanite zone. Moderate amounts of excess Ar shown by biotite grains with ages of 46 to 94 Ma at metamorphic grades up to the high-grade part of the kyanite zone probably represent incomplete degassing during metamorphism. In contrast, the high-grade part of the kyanite zone yields biotite ages of 130 to 197 Ma. The spatial distribution of these older ages in the kyanite zone along the sillimanite zone boundary suggests they reflect trapped excess argon that migrated from higher-grade regions. The most likely source is muscovite that decomposed to form sillimanite. The zone with extreme amounts of excess argon preserves trapped remnants of an 'excess argon wave'. We suggest this corresponds to the area where biotite cooled below its closure temperature in the presence of an elevated Ar wave. Extreme excess Ar is not recognized in muscovite suggesting that the entrapment of the argon wave by biotite took place when the rocks had cooled down to temperatures lower than the closure temperature of muscovite. The breakdown of phengite during ultrahigh-pressure (UHP) metamorphism may be a key factor in accounting for the very old apparent ages seen in many UHP metamorphic regions. This is the first documentation of a regional Ar-wave spatially associated with regional metamorphism. This study also implies that resetting of the Ar isotopic systems in micas can require temperatures up to 600°C; much higher than generally thought.

Key words: $^{40}Ar/^{39}Ar$ analyses, Barrovian type metamorphism, closure temperature, Eastern Tibet, excess argon wave, Longmenshan orogenic belt.

INTRODUCTION

Potassium-bearing minerals such as biotite and muscovite are widely used as target minerals in K-Ar and Ar-Ar geochronology. One of the

*Correspondence.

Received 5 April 2007; accepted for publication 17 October 2008.

doi:10.1111/j.1440-1738.2009.00668.x

assumptions in applying such methods to metamorphic rocks is that above a certain temperature all the accumulated Ar gas will be released from the host mineral and dispersed into the surrounding rocks. After cooling sufficiently, radiogenic argon will again build up in the host mineral. The fate of the released gas is also considered in several studies, particularly in high-pressure metamorphic terrains (Foland 1983; Scaillet 1996; Kelley 2002; Sherlock & Kelley 2002). These studies show that under some circumstances the Ar may be reabsorbed into the host mineral resulting in heterogeneous Ar distribution on the grain scale. Many studies have shown an essentially random distribution of excess argon on a regional scale, but a few examples of pulse or wave-like patterns of released (excess or extraneous) argon have been recognized associated with structural discontinuities (Wanless *et al.* 1970; Smith *et al.* 1994; Shibata *et al.* 1996) and in the vicinities of structural discontinuities or igneous contacts (Hyodo & York 1993). The reported distribution of Ar could be referred to as a 'front' or a 'wave'. Here we use the term 'wave' following the usage of Hyodo and York (1993). Regions that preserve the Ar-wave are spatially limited zones characterized by very old and geologically anomalous apparent Ar ages.

Hyodo and York (1993) present the clearest documented example of an Ar wave that is related to metamorphism. These workers examined the boundary region between a mafic dyke and its country rock and showed that it had become impregnated with 'excess' radiogenic argon. The heat released during the cooling of a mafic dyke (570 Ma) caused intensive degassing of radiogenic argon accumulated in the minerals of the 1000 Ma country rock; the most abundant of these Ar source minerals is K-feldspar, which also has the lowest closure temperature. Hyodo and York (1993) suggest that as a result of this degassing the local ambient argon partial pressure was maintained at a high level for a prolonged period. This excess argon eventually became trapped in the biotite of the contact aureole. The contact metamorphism is developed around an obliquely intruded dyke and the excess argon wave is most clearly recorded in metamorphic biotite from rocks that are located within a distance of 8 m from the upper dyke contact and 20 m from the lower dyke contact. These regions give anomalously old age estimates with maxima of 1400 Ma and 1300 Ma, respectively.

Although local examples of excess argon waves have been recognized, it is as yet not clear if this phenomenon can take place on larger crustal scales and if regional metamorphism may also be related to similar phenomena. Recently, Itaya *et al.* (2005) reported that kyanite grains from river sand, northeast Japan have extremely high excess argon contents up to 1.7×10^{-3} ccSTP/g, and yield apparent ages three times older than the age of the earth. These authors postulated that the kyanites might have recrystallized in host rocks under conditions of ultra-high argon pressure derived from radiogenic argon of potassium-rich phases such as phengite and released during a Barrovian type overprint on a higher-pressure metamorphic event. This type of kyanite may be the result of regional metamorphism in the presence of regionally distributed excess argon.

During the systematic $^{40}Ar/^{39}Ar$ dating of biotite in the Barrovian type metamorphism of the Danba region in the Longmenshan Orogen (also known as the Songpan Ganze Orogen) in the eastern Tibetan plateau (Burchfiel *et al.* 1995; Huang *et al.* 2003a; Wallis *et al.* 2003), we recognized a spatially limited zone within the kyanite zone that yields apparent biotite Ar ages three times older than the metamorphic age found in the high-grade part of the higher-grade sillimanite zone. Here we report the results of $^{40}Ar/^{39}Ar$ analyses of biotite and muscovite from this region of Barrovian type metamorphism and demonstrate a spatial relationship between the excess Ar distribution and the metamorphic zonation. These results imply the existence of a regional excess argon wave in the crust with major implications for the dating of high-grade Barrovian-type and UHP metamorphic belts where temperatures are high enough to cause break down of phengite. Our results also suggest the temperature needed to reset the Ar-isotopic system in previously formed biotite and muscovite can be significantly higher than generally thought.

OUTLINE OF GEOLOGY

The Barrovian type metamorphic belt studied is situated in the Danba area in the central part of Longmenshan orogenic belt in the east of the Tibetan plateau. The Longmenshan region consists of Triassic flysch (Songpan Ganze Flysch) and older sediments deposited on the western fringe of the Proterozoic Yangtze craton (Burchfiel *et al.* 1995). The Danba area consists mainly of Sinian to Triassic metasediments (BGMRSP 1991) and has undergone Barrovian type metamorphism: the

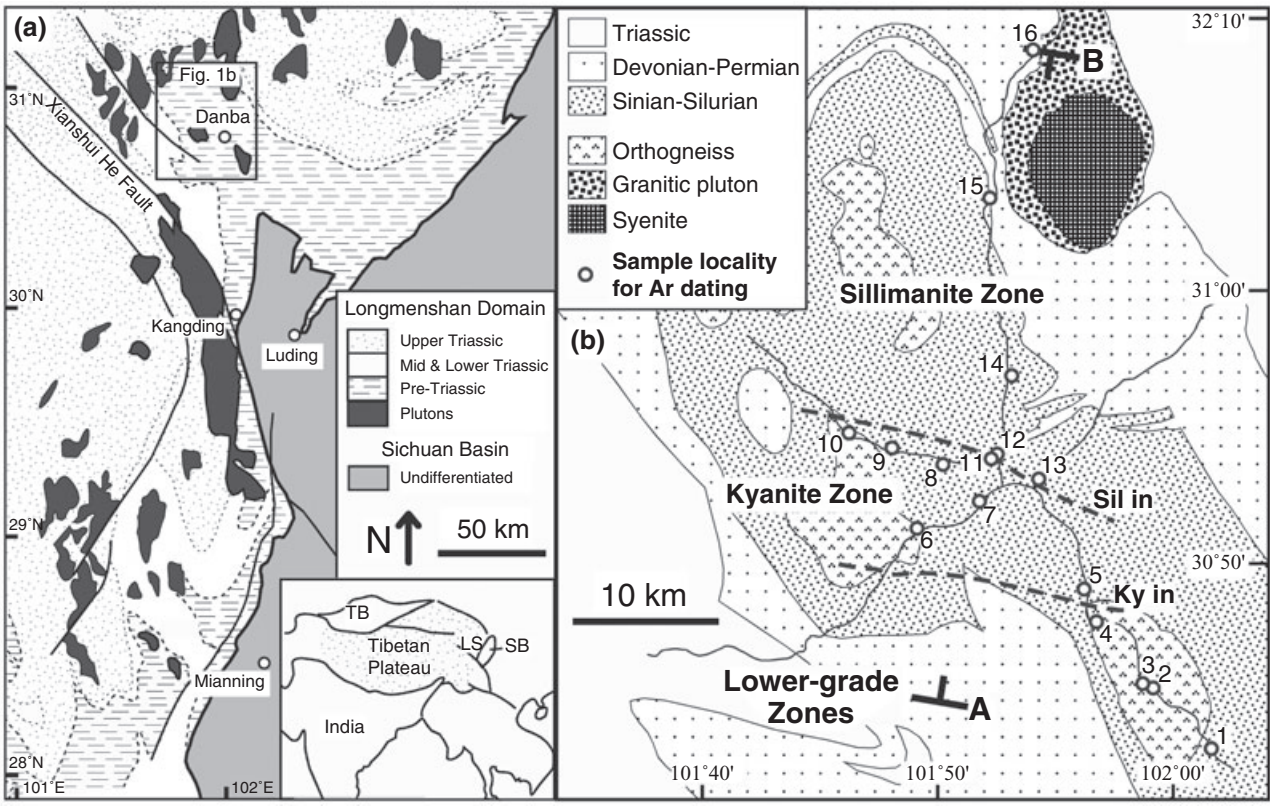

Fig. 1 Simplified geological map (a) of Longmenshan region (after Burchfiel *et al.* 1995) and geological map (b) of the Danba area, showing the location of samples studied. LS: Longmenshan, SB: Sichuan Basin, TB: Tarim basin in (a). Grt: Garnet, Ky: Kyanite, Sil: Sillimanite in (b).

pelitic lithology progressively changes from chlorite-grade slates into sillimanite-K-feldspar schists (Fig. 1) (Huang *et al.* 2003a; Wallis *et al.* 2003) and estimated peak pressure-temperature (P-T) conditions of the sillimanite zone are ca. 480–630 MPa and 640–680°C (Huang *et al.* 2003a). The region has undergone a phase of penetrative ductile deformation, D1, with a NNW–SSE oriented stretching lineation and a top-to-the-S sense of shear, local D2 deformation and a stronger phase of deformation, D3, that formed folds with subhorizontal north-south-oriented axes and steep axial planes (Wallis *et al.* 2003). During D3, a ductile east–west shortening of 10–50% took place. Plutonic rocks have also been deformed and metamorphosed. Electron microprobe (CHIME) monazite dating in the metapelite and sensitive high mass-resolution ion microprobe (SHRIMP) U-Pb dating of apatite in the metamorphosed granodiorite both from the sillimanite zone give compatible ages of ca. 65 Ma. Wallis *et al.* (2003) interpret this as the age of sillimanite grade metamorphism. Wallis *et al.* (2003) have also recognized the existence of old rocks in the Danba, Dahebian and Xinduqiao areas from zircon U-Pb ages (771, 178 and 196 Ma, respectively). These ages suggest that the Longmenshan orogenic belt consists of diverse lithologies predating the Barrovian type metamorphism (ca. 65 Ma). In contrast, the radiometric ages reported by Huang *et al.* (2003b) from the same area show a great range: 159–195 Ma for monazite U-Th-Pb ages, 161–166 Ma for titanite U-Pb ages, 138–204 Ma for Sm-Nd garnet ages, 37–138 Ma for muscovite Rb-Sr ages and 26–118 Ma for biotite Rb-Sr ages. These authors interpret the oldest U-Th-Pb monazite and Sm-Nd garnet ages as constraining an early Barrovian metamorphism (M1) in the interval of 204–190 Ma. Furthermore, these authors suggest a combination of U-Th-Pb monazite and titanite and Sm-Nd garnet ages (168–158 Ma) record a second higher-grade sillimanite grade metamorphic event (M2). On the basis of selected Rb-Sr muscovite (138–100 Ma) and biotite (34–24 Ma) ages these authors also suggest that the area underwent extremely slow cooling after M2 over a period of some 150 m.y. Slow cooling over a period in excess of 150 million years is also suggested by Kirby *et al.* (2002). More complex thermal histories associated with partial resetting of earlier established isoto-

pic ratios are, however, also possible and the strong clustering of biotite Rb-Sr ages around 30 Ma for the whole Danba region (Huang *et al.* 2003b) points to the presence of a younger thermal event such as that proposed by Wallis *et al.* (2003). The results presented in this contribution lend strong support to the idea that there was a widespread Cenozoic thermal event in the Danba area. Our work highlights the problems of both inherited argon and the previously largely unrecognized issue of a regional argon wave when applying K-Ar and $^{40}Ar/^{39}Ar$ dating to polymetamorphic terranes.

$^{40}Ar/^{39}Ar$ ANALYSES

$^{40}Ar/^{39}Ar$ analyses of 27 biotite and muscovite grains were carried out with the laser step-heating. Each grain was placed in a 2 mm drill hole on an aluminum tray. Grains of the age standard 3g hornblende (Roddick 1983), and standards for Ca and K corrections ($CaSi_2$ and synthetic $KAlSi_3O_8$ glass) were also set in the same tray. The trays were subsequently vacuum-sealed in a quartz tube. Neutron irradiation of the samples was carried out in the core of a 5 MW Research Reactor at Kyoto University (KUR) for 8 h using the hydraulic rabbit facility. The fast neutron flux density is 3.9×10^{13} n/cm^2/s and is confirmed to be uniform in the dimension of the sample holder ($\phi 16 \times 15$ mm) as little variation in J-values of the evenly spaced age standards was observed (Hyodo *et al.* 1999). Averaged J-values, potassium and calcium correction factors are $J = 0.02343 \pm 0.00004$, $(40/39)K = 0.0291 \pm 0.0034$, $(36/37)Ca = 0.000242 \pm 0.000015$ and $(39/37)Ca = 0.000580 \pm 0.000040$, respectively.

Each mica grain (ca. 0.5 mm in size) was stepwise-heated using a 5 W continuous argon ion laser. Temperatures of samples were monitored by an infrared thermometer with a precision of 3°C in an area of 0.3 mm diameter (Hyodo *et al.* 1995). Biotite crystals were heated under a defocused laser beam at a given temperature for 30 s. In the case of muscovite, heating to temperatures 680–700°C is likely to lead its thermal decomposition to 'dehydroxylate' (Sletten & Onstott 1998). Major release of radiogenic ^{40}Ar occurs at this temperature. Heating time at a fixed laser power was set at 10–20 s. The extracted gas was purified with a SAES Zr-Al getter (St 101) and kept at 400°C for 5 min. Argon isotopes were measured using a custom-made mass spectrometer with a high resolution ($[M/\Delta M] > 400$), which allows separation of hydrocarbon peaks except for mass 36 (Hyodo *et al.* 1994). Typical blanks of extraction lines are 5×10^{-14}, 3×10^{-14}, 3×10^{-14}, 3×10^{-14} and 2×10^{-12} ccSTP for ^{36}Ar, ^{37}Ar, ^{38}Ar, ^{39}Ar and ^{40}Ar, respectively.

Results of integrated ages are shown in Table 1. Errors of the measurements are expressed at the 1σ level. The age errors of the samples do not include the errors in the age standard. The age spectra of representative crystals are shown in Figure 2, which display plateau-like spectra for both biotite and muscovite crystals, and major release (80%) of argon takes place in the mid temperature range with low and uniform Ca/K ratios. All of the other crystals show similar spectra (see Appendix), and no correlation of calcium phases with older ages is observed. In this contribution we are not primarily concerned with geologically meaningful absolute ages – most of the apparent ages reported here do not correspond to any geological event – and a qualitative assessment of plateaus is sufficient for our purposes.

Figure 3a shows the integrated age data plotted along the line shown in Figure 1. This figure clearly demonstrates that the biotite and muscovite grains display consistent ages of ca. 40 Ma in the sillimanite zone higher than 600°C, which can be interpreted as cooling ages after a peak at around 65 Ma. This is also consistent with the ca. 30 Ma biotite Rb-Sr ages of Huang *et al.* (2003b). In contrast, micas from the lower-grade zones that have experienced maximum temperatures less than 600°C show implied ages varying from 46 to 197 Ma except for one biotite of 28 Ma. In particular, the high-grade part of the kyanite zone adjacent to the sillimanite zone (kyanite-sillimanite boundary zone in Fig. 3b) shows extremely old biotite ages, one of which is more than three times the peak age of the sillimanite zone around 65 Ma. Muscovite grains also show a significant variation in ages in the kyanite and lower-grade zones. Coexisting biotite and muscovite in the kyanite-sillimanite boundary zone yield ages of 197 Ma and 64 Ma, respectively (Fig. 2). The presence of apparent ages three times older than the age of a peak metamorphism and biotite ages older than associated muscovite ages clearly show the presence of large amounts of excess argon in the sample.

DISCUSSION

The presence of discordant and anomalously old $^{40}Ar/^{39}Ar$ ages in metamorphic rocks has been

Table 1 Summary of radiometric dating

Outcrop	Sample	Zone	Rock type	Mineral	Method	Age (Ma)	Locality	
1	DBT-23Bt2	Lower grade	Deformed basic dyke	Bt	Ar-Ar	82.2 ± 1.0	N30°42.88′	E102°01.30′
2†	DBT-31Bt1	Lower grade	Deformed granite	Bt	Ar-Ar	52.6 ± 0.7	N30°45.13′	E101°59.18′
2†	DBT-31Bt2	Lower grade	Deformed granite	Bt	Ar-Ar	46.3 ± 0.9		
2†	DBT-31Ms1	Lower grade	Deformed granite	Ms	Ar-Ar	104.3 ± 1.0		
2†	DBT-31Ms2	Lower grade	Deformed granite	Ms	Ar-Ar	86.9 ± 0.7		
3†	DBW-19cBt1	Lower grade	Deformed aplite	Bt	Ar-Ar	89.5 ± 1.1	N30°45.32′	E101°58.90′
3†	DBW-19cBt2	Lower grade	Deformed aplite	Bt	Ar-Ar	94.2 ± 1.5		
3†	DBW-19cMs1	Lower grade	Deformed aplite	Ms	Ar-Ar	70.8 ± 0.7		
4†	DBT-41Bt	Lower grade	Deformed granite	Bt	Ar-Ar	84.1 ± 0.7	N30°47.65′	E101°56.83′
5	DBT-43Bt	Ky	Pelitic schist	Bt	Ar-Ar	83.1 ± 0.9	N30°48.75′	E101°56.18′
6†	DBA-27Bt	Ky	Deformed granite	Bt	Ar-Ar	53.1 ± 0.9	N30°51.37′	E101°49.20′
7	DBA-20Ms	Ky	Qtz-rich vein	Ms	Ar-Ar	74.3 ± 1.0	N30°52.34′	E101°51.86′
8	DBK-24Bt	Ky	Pelitic schist	Bt	Ar-Ar	28.3 ± 0.5	N30°53.85′	E101°50.12′
8	DBK-24Ms	Ky	Pelitic schist	Ms	Ar-Ar	102.5 ± 0.9		
9	DBT-09Ms2	Ky	Pegmatite	Ms	Ar-Ar	62.7 ± 1.1	N30°54.23′	E101°48.07′
9	DBT-09Ms	Ky	Pegmatite	Ms	K-Ar	38.3 ± 0.9		
10†	DBT-08Bt	Ky	Deformed granite	Bt	Ar-Ar	71.8 ± 1.7	N30°54.75′	E101°46.07′
11	DBW-19bMs2	Ky-Sill	Pegmatite	Ms	Ar-Ar	79.7 ± 0.9	N30°53.79′	E101°52.16′
11	DBW-19bMs1	Ky-Sill	Pegmatite	Ms	Ar-Ar	54.5 ± 1.3		
12	DBT-67Bt	Ky-Sill	Pelitic schist	Bt	Ar-Ar	132.9 ± 1.2	N30°53.87′	E101°52.43′
12	DBT-67Ms	Ky-Sill	Pelitic schist	Ms	Ar-Ar	47.1 ± 0.8		
13	DBT-71Bt	Ky-Sill	Pelitic schist	Bt	Ar-Ar	197.0 ± 1.6	N30°53.07′	E101°54.18′
13	DBT-71Ms1	Ky-Sill	Pelitic schist	Ms	Ar-Ar	64.4 ± 1.8		
14	DBK-81Bt	Sill	Pelitic schist	Bt	Ar-Ar	40.5 ± 0.5	N30°56.57′	E101°52.88′
14	DBK-81Ms	Sill	Pelitic schist	Ms	Ar-Ar	35.1 ± 1.0		
15	DBT-61Bt	Sill	Pelitic schist	Bt	Ar-Ar	39.7 ± 0.7	N31°03.40′	E101°52.05′
15‡	DBT-63	Sill	Pelitic schist	Mon	CHIME	65 ± 3		
16	DBT-53Bt	Sill	Deformed granite	Bt	Ar-Ar	36.6 ± 0.8	N31°08.98′	E101°54.25′
16‡	DBT-51	Sill	Deformed granite	Apa	SHRIMP	67 ± 12		
16†	DBT-51Bt	Sill	Deformed granite	Bt	Ar-Ar	52.2 ± 0.5		

† Ar-Ar age spectra presented in data repository of Wallis *et al.* (2003).

‡ Age data taken from Wallis *et al.* (2003).

$^{40}Ar/^{39}Ar$ integrated ages of biotite (Bt) and muscovite (Ms) grains from Barrovian type metamorphic belt in the Danba area, eastern Tibet. One K-Ar age of muscovite from pegmatite vein is also shown in this table. Sample locations are seen in Figure 1. CHIME monazite (Mon) age (65 Ma) and SHRIMP apatite (Apa) age (67 Ma) are after Wallis *et al.* (2003).

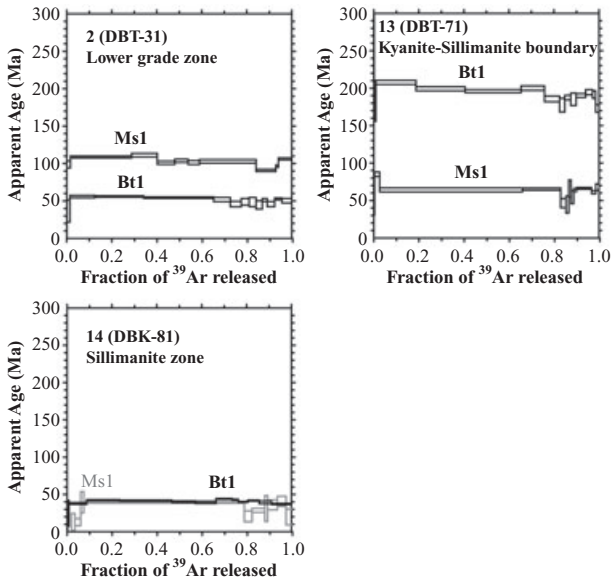

Fig. 2 $^{40}Ar/^{39}Ar$ age spectra of representative biotite and muscovite grains from Barrovian type metamorphic belt in the Danba area, eastern Tibet.

widely reported. Examples are the Dora Maira massif, Italy (Arnaud & Kelley 1995; Scaillet 1996), the Su-Lu and Dabie areas, China (Li *et al.* 1994; Giorgis *et al.* 2000), the Kaghan valley area, Pakistan (Tonarini *et al.* 1993), the Tso Morari Complex, western Himalaya, India (Gouzu *et al.* 2006a), the Gourma area, Mali (Jahn *et al.* 2001), the Sesia-Lanzo zone, Italy (Ruffet *et al.* 1995, 1997; Inger *et al.* 1996), the Tavsanli Zone, Turkey (Sherlock & Arnaud 1999), and the Betic Zone, Spain (De Jong *et al.* 2001). These results are likely due to the presence of excess ^{40}Ar trapped in the metamorphic minerals during the metamorphism. Many of these examples are from areas of ultrahigh-pressure metamorphism.

The excess ^{40}Ar may have several origins. De Jong *et al.* (2001) show the relationship between the secondary fluid infiltration and discordant age. They argued that the excess ^{40}Ar is contained in submicroscopic illite in the phengites identified by TEM analyses, though Giorgis *et al.* (2000) could not find any apparent interlayer phase in the phengite showing discordant age relationships. On the other hand, continental materials like the Dora Maira massif (e.g. Chopin 1984; Schertl *et al.* 1991) have experienced polymetamorphism and to some extent may retain radiogenic ^{40}Ar inherited from the protolith; this would produce discordant ages if there was incomplete degassing and incomplete resetting of minerals during metamorphism (Gouzu *et al.* 2006b). In addition to incomplete degassing, we suggest there is a problem caused by the presence of an excess argon wave with extreme Ar concentrations formed in mica that cooled below its closure temperature in the presence of an Ar-wave (Fig. 4). This phenomenon has not been recognized by these previous researchers probably because they have not carried out the systematic sample collection and dating along traverses from low to high-grade zones in the belt.

The results of our detailed sampling, age determination, and comparison with metamorphic grade clearly show the presence of a zone of trapped excess argon that results in very old apparent ages. Averaged values of biotite and muscovite ages for four zones (Fig. 3b), in increasing metamorphic temperature, show a gradual decrease towards the sillimanite zone. These data may be accounted for by an overall increase in degassing and decrease in inherited Ar in the micas from these regions with increasing metamorphic temperature. There is, however, an exception to this trend shown clearly by the extremely old biotite ages (130 to 197 Ma; Fig. 3) in the kyanite-sillimanite boundary zone. In addition, in this zone, muscovite may record a younger apparent age than biotite in conflict with the generally observed relationships (Fig. 3b). These relationships cannot be accounted for by progressive degassing with increasing temperature, because the biotite ages of 130 to 197 Ma are significantly older than both biotite ages of lower-grade zones (46 to 94 Ma) and muscovite ages from the same kyanite-sillimanite boundary zone (Fig. 3). In our interpretation, biotite grains with ages of 130 to 197 Ma in the kyanite-sillimanite boundary zone trapped excess argon derived from an argon wave zone. This excess argon was probably derived from the resetting of potassium bearing minerals in the sillimanite zone. The most likely candidate for a source mineral is muscovite, which decomposes by the reactions $St + Ms + Qtz = Sil + Grt + Bt + H_2O$ and $Ms + Qtz = Sil + Kfs + H_2O$. In the sillimanite zone, muscovite also exists, but its modal proportion decreases from the south to the north (Huang *et al.* 2003a), suggesting that the former reaction proceeded extensively in the sillimanite zone and the latter one in the higher-grade zone. We propose that muscovite decomposition in this region resulted in the release of the contained Ar and lead to the formation of an excess argon wave, which migrated to the lower-grade zones at the structurally higher level than the sillimanite zone. A similar type of age profile is reported by Baxter *et al.* (2002), but in this case it is related to

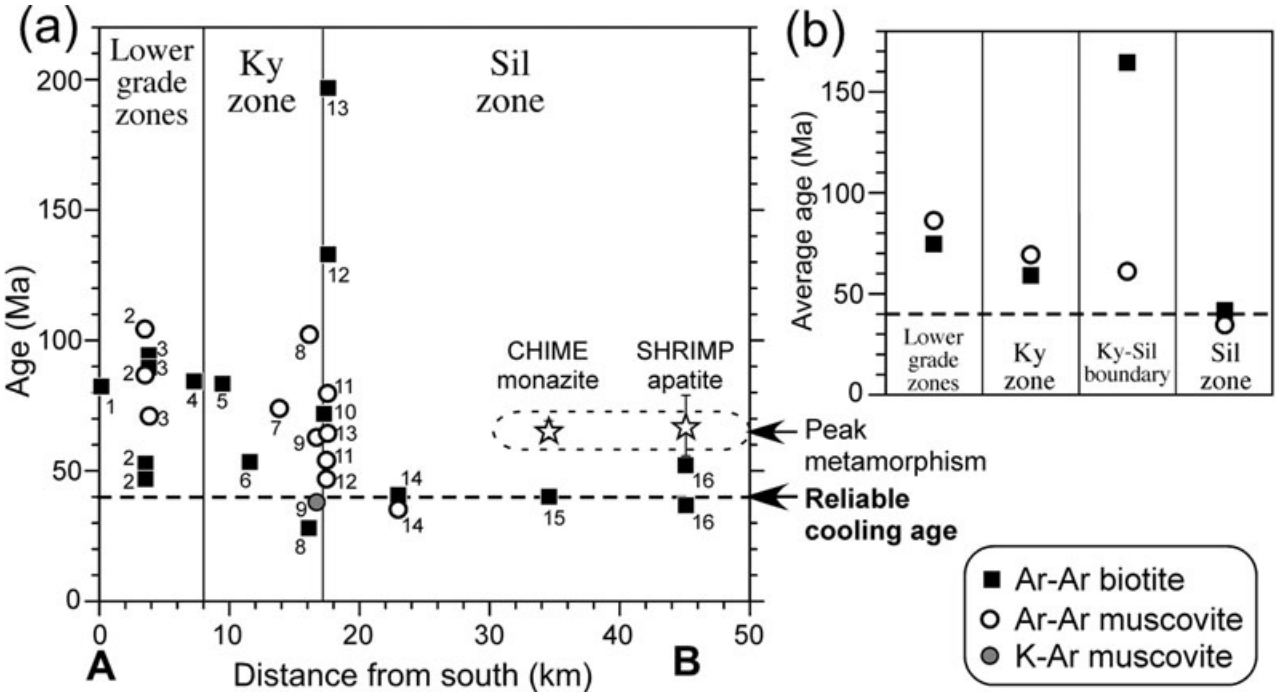

Fig. 3 (a) $^{40}Ar/^{39}Ar$ integrated age data plotted along the line shown in Figure 1(b), in which CHIME monazite age (65 Ma) and sensitive high mass-resolution ion microprobe (SHRIMP) apatite age (67 Ma) are after Wallis *et al.* (2003). Corresponding outcrop numbers (1–16; Fig. 1) are also shown for each datum. (b) Averages of $^{40}Ar/^{39}Ar$ biotite and muscovite ages calculated for the four zones, lower-grade zones (1–4), kyanite zone (5–10), kyanite-sillimanite boundary zone (11–13) and sillimanite zone (14–16).

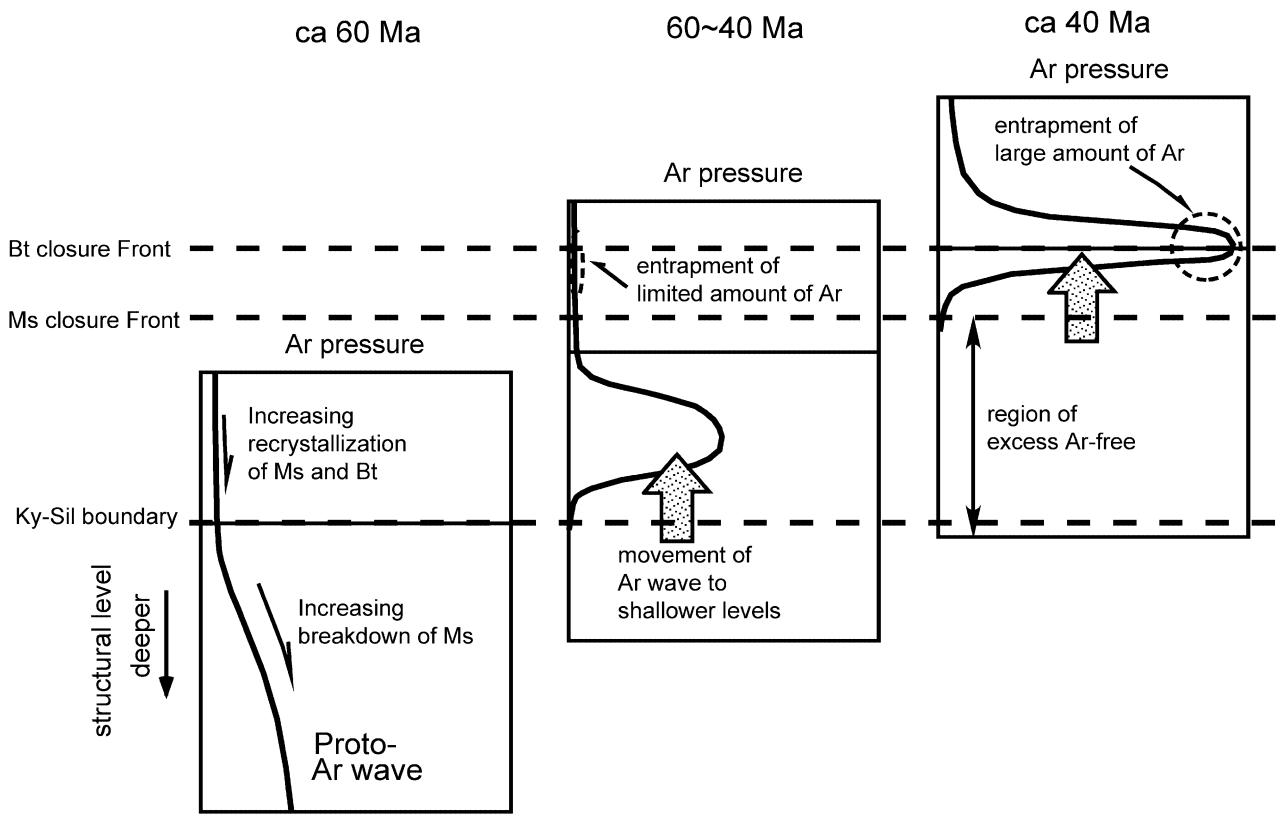

Fig. 4 Schematic diagram showing three stages in the development of the envisaged Ar wave and its preservation in biotite.

differences in diffusion characteristics in contrasting lithologies. In the Danba region the presence of the Ar wave does not correspond to any clear lithological or structural boundary.

Coexisting biotite and muscovite in the high-grade part of the kyanite zone in the Danba area give ages of 197 Ma and 64 Ma, respectively. This suggests that the trapping of argon by biotite in the excess argon wave took place when the rocks cooled down to the temperatures lower than the closure temperature of muscovite but not below that of biotite (Fig. 4). We suggest biotite (46 to 94 Ma) in the lower-grade zones did not completely degas during metamorphism and retains moderate amounts of excess argon inherited from the host lithologies.

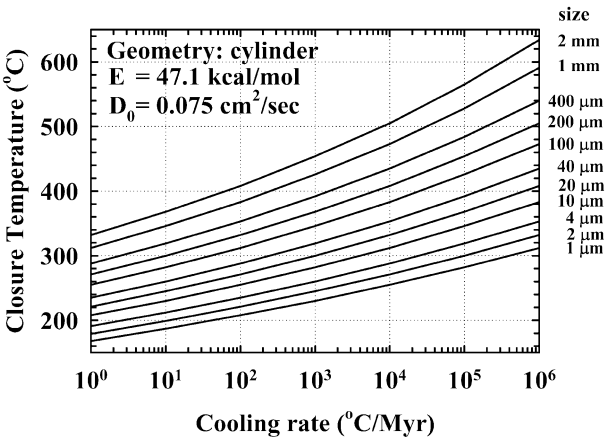

Fig. 5 Variation of biotite closure temperature (°C), for different grain sizes and cooling rates based on the diffusion model by Dodson (1973) using parameters for biotite by McDougall and Harrison (1999). E and D_0 denote an activation energy and a frequency factor, respectively. The grain size is the diameter of a cylindrical grain. This geometry is appropriate for modeling the diffusion behavior of mica, because of the rapid diffusion perpendicular to the c-axis.

IMPLICATIONS OF PRESENT STUDY

The presence of this type of excess argon wave has been hitherto unreported and has major implications for the type of rocks likely to be most strongly affected by excess argon and, therefore, unsuitable for Ar-based radiometric dating. Our work also has implications for estimates of appropriate closure (or resetting) temperatures for biotite and muscovite.

The closure temperatures of biotite and muscovite have long been believed to be 300°C and 350°C, respectively, since the work of Purdy and Jäger (1976). In the last decade, some geochronologists have cast doubt on the closure temperatures proposed by Purdy and Jäger (1976) in their argon analyses of biotite and muscovite (cf., Gouzu *et al.* 2006a,b). Villa (1998) examined Jäger's calibration of the closure (or blocking) temperatures and proposed new closure temperatures of 500°C for muscovite and 450°C for biotite. Takeshita *et al.* (2004) who studied the resetting temperature of detrital white micas based on the systematic K-Ar analyses of phengites in the calcschists along the Chisone valley in western Alps by Takeshita *et al.* (1994) strongly support the new closure temperature proposed by Villa (1998). We also carried out $^{40}Ar/^{39}Ar$ analyses of biotites and muscovites from the area studied as seen in Figures 2 and 3. Coexisting biotite and muscovite in the sillimanite zone with metamorphic temperatures exceeding 600°C give consistent cooling ages of ca. 40 Ma (Fig. 2). However, biotite and muscovite in the lower-grade zones with peak metamorphic temperatures below 500°C give discordant ages (Figs 2,3), even if the 'spike' of the $^{40}Ar/^{39}Ar$ apparent ages at the boundary between kyanite and sillimanite zones are excluded. Diffusion modeling shows large grain size and rapid cooling can also lead to higher closure temperatures (Fig. 5). However, to account for the observed changes in the present study would require mica grains with a width in excess of 1.2 mm and a cooling rate faster than 1°C/yr. In the study area the mica grain size is variable, but does not much exceed 0.5 mm in any of the analysed samples. In addition, the difference between peak and cooling ages suggests a relatively slow cooling of 10^{-5}°C/yr. There is, therefore, no evidence that grain size or cooling rate played a role in raising the closure temperature of mica in the present area. These results suggest that muscovite and biotite in polymetamorphic terranes, such as in the present study, require higher metamorphic temperatures to completely reset the Ar isotopic system than generally thought.

One approach to successfully estimate the cooling age of metamorphic rocks using K-Ar and $^{40}Ar/^{39}Ar$ muscovite and biotite analyses is to focus on rocks that have a simple metamorphic history and do not have problems with inherited argon. Suitable material is likely to be oceanic rather than continental in origin (Gouzu *et al.* 2006b).

Selection of rocks with a simple metamorphic history can assist in obtaining reliable dates from Ar-based radiometric dating. However, the second problem highlighted in this study: the presence of a regional Ar-wave that migrates some distance through the crust may still pose serious problems.

Which sort of rock is most likely to be affected? Our study suggests that an argon wave is likely to form whenever there is widespread breakdown of potassium-bearing minerals. The greater the time difference between the formation of these minerals and their breakdown the more time there is for Ar to build up resulting in a larger Ar wave. The boundary region between the Kyanite and Sillimanite zones in Barrovian type metamorphism and high-temperature zones in low-P/T type metamorphism are generally associated with the breakdown of muscovite, a major potassium-bearing mineral in many rock types. This boundary region is, therefore, likely to be associated with an Ar wave in many cases and Ar-dating from this region should be interpreted with caution.

Many of the reported cases of extreme excess argon causing problems with Ar-based dating are in UHP rocks (Tonarini *et al.* 1993; Li *et al.* 1994; Arnaud & Kelley 1995; Scaillet 1996; Giorgis *et al.* 2000; Gouzu *et al.* 2006a). Can this phenomenon also be explained in terms of an Ar-wave? Several recent studies have suggested that partial melting has occurred in UHP domains and this may be a key factor controlling the exhumation of such rocks (e.g. Hermann *et al.* 2001; Wallis *et al.* 2005). Such melting is likely to involve breakdown of phengite (e.g. Patiño Dounce & McCarthy 1998), which will release any trapped Ar. This breakdown could result in the formation of localized high Ar contents in the melt and its release to the overlying rocks may account for the commonly observed very high amounts of excess Ar and extremely old apparent ages in many UHP rocks. We speculate that the extremely high-excess argon bearing kyanites reported by Itaya *et al.* (2005) may have a similar origin.

CONCLUSIONS

Laser step heating $^{40}Ar/^{39}Ar$ analysis of single crystals of biotite and muscovite in the metamorphic rocks collected systematically from a Barrovian type metamorphic belt, eastern Tibet, reveal that the biotites in the kyanite-grade zone record the presence of an excess argon wave. The spatial relationship with the metamorphic zonation suggests this developed after the decomposition of muscovite in the sillimanite zone. This type of excess argon wave has been hitherto unreported and suggests that rocks surrounding a region that has experienced widespread breakdown of K-bearing minerals are unlikely to give reliable age data by Ar dating. In addition, the breakdown of phengite during partial melting of UHP rocks could be a key factor in accounting for the very old apparent K-Ar and $^{40}Ar/^{39}Ar$ ages seen in many UHP metamorphic regions. The $^{40}Ar/^{39}Ar$ analysis also yielded consistent cooling ages of ca 40 Ma in the sillimanite zone with peak metamorphic temperatures higher than 600°C and discordant ages in the zones with peak temperatures lower than 600°C. This suggests the temperatures needed to reset Ar isotopic systems in micas are significantly higher than generally thought.

ACKNOWLEDGEMENTS

We thank Ms Yuko Takeshima for her help with Ar analyses. The results presented here are part of a project supported by a Grant-in-Aid awarded to S. Wallis (Grant No. 13573011). Sample preparation for age determination was carried out in part under the Visiting Researchers Program at the Kyoto University Reactor Institute.

REFERENCES

ARNAUD N. O. & KELLEY S. P. 1995. Evidence for excess Ar during high pressure metamorphism in the Dora Maira (western Alps, Italy), using a Ultra-Violet Laser Ablation Microprobe ^{40}Ar-^{39}Ar technique. *Contributions to Mineralogy and Petrology* **121**, 1–11.

BAXTER E. F., DEPAOLO D. J. & RENNE P. J. 2002. Spatially correlated anomalous $^{40}Ar/^{39}Ar$ 'age' variations in biotites about a lithologic contact near Simplon Pass, Switzerland: A mechanistic explanation for excess Ar. *Geochimica et Cosmochimica Acta* **66**, 1067–83.

BURCHFIEL B. C., ZHILIANG C., YUPING L. & ROYDEN L. H. 1995. Tectonics of the Longmen Shan and adjacent regions, central China. *International Geology Review* **37**, 661–735.

BUREAU OF GEOLOGY AND MINERAL RESOURCES OF SICHUAN PROVINCE. 1991. *Regional Geology of Sichuan Province*. Geological Publishing House, Beijing (in Chinese with English summary).

CHOPIN C. 1984. Coesite and pure pyrope in high-grade blueschists of the western Alps; A first record and some consequences. *Contributions to Mineralogy and Petrology* **86**, 107–18.

DE JONG K., FÉRAUD G., RUFFET G., AMOURIC M. & WIJBRANS J. R. 2001. Excess argon incorporation in phengite of the Mulhacén Complex: Submicroscopic illitization and fluid ingress during late Miocene extension in the Betic Zone, south-eastern Spain. *Chemical Geology* **178**, 159–95.

DODSON M. H. 1973. Closure temperature in cooling geochronological and petrological systems. *Contributions to Mineralogy and Petrology* **40**, 259–74.

FOLAND K. A. 1983. $^{40}Ar/^{39}Ar$ incremental heating plateaus for biotites with excess argon. *Isotope Geoscience* **1**, 3–21.

GIORGIS D., COSCA M. & LI S. 2000. Distribution and significance of extraneous argon in UHP eclogite (Sulu terrain, China): Insight from in situ $^{40}Ar/^{39}Ar$ UV laser ablation analysis. *Earth and Planetary Science Letter* **181**, 605–15.

GOUZU C., ITAYA T., HYODO H. & AHMAD T. 2006a. Cretaceous isochron ages from K-Ar and Ar-Ar dating of eclogitic rocks in the Tso Morari complex, western Himalaya, India. Gondwana. *Research* **9**, 426–40.

GOUZU C., ITAYA T., HYODO H. & MATSUDA T. 2006b. Excess ^{40}Ar-free phengite in ultrahigh-pressure metamorphic rocks from the Lago di Cignana area, Western Alps. *Lithos* **92**, 418–30.

HERMANN J., RUBATTO D., KORSAKOV A. & SHATSKY V. S. 2001. Multiple zircon growth during fast exhumation of diamondiferous deeply subducted continental crust. *Contributions to Mineralogy and Petrology* **141**, 66–82.

HUANG M. H., BUICK I. S. & HOU L. W. 2003a. Tectonometamorphic evolution of the eastern Tibet plateau: Evidence from the central Songpan – Garze orogenic belt, western China. *Journal of Petrology* **44**, 255–78.

HUANG M. H., MAAS R., BUICK I. S. & WILLIAMAS I. S. 2003b. Crustal response to continental collisions between the Tibet, Indian, South China and North China Blocks: Geochronological constraints from the Songpan-Garze orogenic belts, western China. *Journal of Metamorphic Geology* **21**, 223–40.

HYODO H. & YORK D. 1993. The discovery and significance of a fossilized radiogenic argon wave (argonami) in the earth's crust. *Geophysical Research Letter* **20**, 61–4.

HYODO H., ITAYA T. & MATSUDA T. 1995. Temperature measurement of small minerals and its precision using Laser heating. *Bulletin of Research Institute of Natural Sciences, Okayama University of Science* **21**, 3–6 (in Japanese with English Abstract).

HYODO H., KIM S., ITAYA T. & MATSUDA T. 1999. Homogeneity of neutron flux during irradiation for $^{40}Ar/^{39}Ar$ age dating in the research reactor at Kyoto University. *Journal of Mineralogy, Petrology and Economic Geology* **94**, 329–37.

HYODO H., MATSUDA T., FUKUI S. & ITAYA T. 1994. $^{40}Ar/^{39}Ar$ age determination of a single mineral grain by laser step heating. *Bulletin of Research Institute of Natural Sciences, Okayama University of Science* **20**, 63–7 (in Japanese with English abstract)

INGER S., RAMSBOTHAM W., CLIFF R. A. & REX D. C. 1996. Metamorphic evolution of the Sesia-Lanzo zone, Western Alps: Time constraints from multi-system geochronology. *Contributions to Mineralogy and Petrology* **126**, 152–68.

ITAYA T., HYODO H., URUNO K. & MIKOSHIBA M-U. 2005. Ultra-high excess argon in kyanites: Implications for ultra-high pressure metamorphism in Northern Japan. *Gondwana Research* 8, 617–21.

JAHN B., CABY R. & MONIE P. 2001. The oldest UHP eclogites of the World: Age of UHP metamorphism, nature of protoliths and tectonic implications. *Chemical Geology* **178**, 143–58.

KELLEY S. 2002. Excess argon in K–Ar and Ar–Ar geochronology. *Chemical Geology* **188**, 1–22.

KIRBY E., REINERS P. W., KROL M. A., WHIPPLE K. X., HODGES K. V. & FARLEY K. A. 2002. Late cenozoic evolution of the eastern margin of the Tibetan plateau: Inferences from $^{40}Ar/^{39}Ar$ and U-Th/He thermochronology. *Tectonics* **21**, 1–20.

LI S., WANG LI S., CHEN S. *et al.* 1994. Excess argon in phengite from eclogite: Evidence from dating of eclogite minerals by Sm-Nd, Rb-Sr and $^{40}Ar/^{39}Ar$ methods. *Chemical Geology* **112**, 343–50.

MCDOUGALL I. & HARRISON T. M. 1999. *Geochronology and Thermochronology by the $^{40}Ar/^{39}Ar$ Method*, 2nd edn. Oxford University Press, Oxford.

PATIÑO DOUNCE A. E. & MCCARTHY T. C. 1998. Melting of crustal rocks during continental collision and subduction. *In* Hacker B. R. & Liou J. G. (eds.) *When Continents Collide*, pp. 27–55. Kluwer Academic, Dordrecht.

PURDY J. W. & JÄGER E. 1976. K-Ar ages on rock-forming minerals from the central Alps. *Memoirs of the Institute of Geology and Mineralogy, University of Padova* **30**, 3–31.

RODDICK J. C. 1983. High precision intercalibration of ^{40}Ar-^{39}Ar standards. *Geochimica Cosmochimica Acta* **47**, 887–98.

RUFFET G., FÉRAUD G., BALLÉVRE M. & KIÉNAST J. R. 1995. Plateau ages and excess argon in phengites: An ^{40}Ar-^{39}Ar laser probe study of Alpine micas (Sesia zone, Western Alps, northern Italy). *Chemcal Geology* **121**, 327–43.

RUFFET G., GRUAU G., BALLÉVRE M., FÉRAUD G. & PHILIPPOT P. 1997. Rb-Sr and ^{40}Ar-^{39}Ar laser probe dating of high-pressure phengites from the Sesia zone (Western Alps): Underscoring of excess argon and new age constraints on the high-pressure metamorphism. *Chemical Geology* **41**, 1–18.

SCAILLET S. 1996. Excess ^{40}Ar transport scale and mechanism in high-pressure phengites: A case study from an eclogitized metabasite of the Dora-Maira nappe, western Alps. *Geochimica et Cosmochimica Acta* **60**, 1075–90.

SCHERTL H. P., SCHREYER W. & CHOPIN C. 1991. The pyrope-coesite rocks and their country rocks at Parigi, Dora Maira Massif, Western Alps; Detailed petrography, mineral chemistry and PT-path. *Contributions to Mineralogy and Petrology* **108**, 1–21.

SHERLOCK S. C. & ARNAUD N. O. 1999. Flat plateau and impossible isochrons: Apparent ^{40}Ar-^{39}Ar geochronology in a high-pressure terrain. *Geochimica et Cosmochimica Acta* **63**, 2835–8.

SHERLOCK S. C. & KELLEY S. P. 2002. Excess argon in HP-LT rocks: A UV laserprobe study of phengite and K-free minerals. *Chemical Geology* **182**, 619–36.

SHIBATA K., SUWA K., UCHIUMI S. & AGATA T. 1996. Excess Ar in biotites from the Broderick Falls (Webuye) area, western Kenya: Implications for the tectonothermal history of the Mozambique Belt and its Archeaean foreland. *Journal of African Earth Science* **23**, 433–41.

SLETTEN V. W. & ONSTOTT T. C. 1998. The effect of the instability of muscovite during in vacuo heating on ^{40}Ar/^{39}Ar step-heating spectra. *Geochimica et Cosmochimica Acta* **62**, 123–41.

SMITH P. E., YORK D., EASTON R. M., ÖZDEMIR Ö. & LAYER P. W. 1994. A laser ^{40}Ar-^{39}Ar study of minerals across the Grenville Front: Investigation of reproducible excess Ar patterns. *Canadian Journal of Earth Sciences* **31**, 808–17.

TAKESHITA H., GOUZU C. & ITAYA T. 2004. Chemical features of white micas from the Piemonte calcschists, western Alps and implications for K-Ar ages of metamorphism. *Gondwana Research* **7**, 457–66.

TAKESHITA H., SHIMOYA H. & ITAYA T. 1994. White mica K-Ar ages of blueschist-facies rocks from the Piemonte 'calcschists' in the western Italian Alps. *Island Arc* **3**, 151–62.

TONARINI S., VILLA I. M., OBERLI F. *et al.* 1993. Eocene age of eclogite metamorphism in Pakistan Himalaya: Implications for India-Eurasian collision. *Terra Nova* **5**, 13–20.

VILLA I. M. 1998. Isotopic closure. *Terra Nova* **10**, 42–7.

WALLIS S. R., TSUBOI M., SUZUKI K., FANNING M., JIANG L. & TANAKA T. 2005. Role of partial melting in the evolution of the Sulu (eastern China) ultrahigh-pressure belt. *Geology* **33**, 129–32.

WALLIS S., TSUJIMORI T., AOYA M. *et al.* 2003. Cenozoic and Mesozoic metamorphism in the Longmenshan orogen: Implications for geodynamic models of eastern Tibet. *Geology* **31**, 745–8.

WANLESS R. K., STEVENS R. D. & LOVERIDGE W. D. 1970. Anomalous parent-daughter isotopic relationships in rocks adjacent to the Grenville Front near Chibougamau, Quebec. *Eclogae Geologicae Helvetiae* **63**, 345–64.

APPENDIX

^{40}Ar/^{39}Ar age and ^{37}Ar/^{39}Ar ratio spectra of biotite and muscovite samples in the Danba area, eastern Tibet. The first number represents the outcrop listed in Table 1. In some samples, the ^{37}Ar/^{39}Ar ratio spectra indicate the presence of different mineral phases other than micas, but they rarely correlate with the age spectra.